MATHEMATICAL BIOSCIENCES
AND ENGINEERING
Volume **13**, Number **5**, October **2016**

doi:10.3934/mbe.2016028

pp. **1011–1041**

MODELING THE ROLE OF HEALTHCARE ACCESS INEQUALITIES IN EPIDEMIC OUTCOMES

Oscar Patterson-Lomba[1] ¶

[1]Harvard T.H. Chan School of Public Health, Department of Biostatistics
Boston, MA, USA

Muntaser Safan [2,3,4*] ¶, Sherry Towers[2] and Jay Taylor[5]

[2] SAL MCMSC, School of Human Evolution and Social Change
Arizona State University, Tempe, AZ, USA
[3] Mathematics Department, Faculty of Science, Mansoura University
Mansoura 35516, Egypt
[4] Department of Mathematical Sciences, Faculty of Applied Sciences
Umm Al-Qura University
21955 Makkah, Saudi Arabia
[5] School of Mathematical and Statistical Sciences
Arizona State University, Tempe, AZ, USA

(Communicated by Christopher M. Kribs)

Abstract. Urban areas, with large and dense populations, offer conditions that favor the emergence and spread of certain infectious diseases. One common feature of urban populations is the existence of large socioeconomic inequalities which are often mirrored by disparities in access to healthcare. Recent empirical evidence suggests that higher levels of socioeconomic inequalities are associated with worsened public health outcomes, including higher rates of sexually transmitted diseases (STD's) and lower life expectancy. However, the reasons for these associations are still speculative. Here we formulate a mathematical model to study the effect of healthcare disparities on the spread of an infectious disease that does not confer lasting immunity, such as is true of certain STD's. Using a simple epidemic model of a population divided into two groups that differ in their recovery rates due to different levels of access to healthcare, we find that both the basic reproductive number ($\mathcal{R}_0$) of the disease and its endemic prevalence are increasing functions of the disparity between the two groups, in agreement with empirical evidence. Unexpectedly, this can be true even when the fraction of the population with better access to healthcare is increased if this is offset by reduced access within the disadvantaged group. Extending our model to more than two groups with different levels of access to healthcare, we find that increasing the variance of recovery rates among groups, while keeping the mean recovery rate constant, also increases $\mathcal{R}_0$ and disease prevalence. In addition, we show that these conclusions are sensitive to how we quantify the inequalities in our model, underscoring the importance of basing analyses on appropriate measures of inequalities. These insights shed light on the possible impact that increasing levels of inequalities in healthcare access can have on epidemic outcomes, while offering plausible explanations for the observed empirical patterns.

2010 *Mathematics Subject Classification.* Primary: 92D25, 92D30; Secondary: 92B99.
Key words and phrases. Urbanization, healthcare access inequalities, epidemic outcomes.

* Corresponding author: Muntaser Safan.

¶ These authors contributed equally to this work.

1. **Introduction.** The world is becoming increasingly urbanized, especially developing countries in Asia and Africa. Today, more than half of the world's population lives in cities, and by mid-century it is expected that this proportion will rise to over 60% [43]. Rapid urbanization can have significant public-health implications [13, 18, 19, 21, 26]. In particular, when combined with poor living conditions and an overburdened public health infrastructure, rapid growth of urban populations can create favorable conditions for the spread of certain infectious and chronic diseases [1, 3, 4, 32, 47].

One common feature of urbanization is the amplification of socioeconomic inequalities among residents. Urban dwellers enjoy, on average, better health, education and income. At the same time, these benefits are usually not evenly distributed across the population [14, 34, 40]. Figure 1 (left) illustrates an example of this phenomenon by showing larger income inequality in households within U.S. Metropolitan Statistical Areas (MSAs) as compared to households outside MSAs. Moreover, recent evidence shows that income inequality has been on the rise in the United States during the past four decades, and wealth inequality is today more extreme than at any time since the Great Depression [39].

Large disparities in economic, social and living conditions can in turn result in inequalities in access to healthcare and other social services, all potentially affecting the *well-being* of individuals. For example, limited access to professional medical attention, vaccination and medication are common challenges for poorer urban residents [26], which can result in the emergence of drug resistance in urban areas in part because of difficulties in adhering to complicated and expensive treatment regimes [10, 12]. The evidence also suggests that within urban areas across the world, wealthier residents have better access to education and mass media, and are more exposed to campaigns for disease prevention (see right panel of Figure 1).

Interplay between inequalities in healthcare access and epidemic outcomes. Empirical evidence suggests that health outcomes are worse in societies with larger income differences [46]. This observation is important because, in many countries, inequalities in health have been increasing [33, 38, 39]. However, in most of these studies, the term 'health' has been equated with 'life expectancy' [11, 45], while other factors, such as infectious diseases (IDs), have not been thoroughly considered.

Additionally, the literature on this topic lacks mechanistic (causal) pathways to explain these statistical findings [46]. Thus an important question arises: why is income inequality, rather than income per-capita, often the factor more strongly associated with worsened health outcomes? Focusing on mortality rates, this association can be explained, at least in part, by observing that although more money can buy better healthcare, this impact is greater for people that are lower on the income distribution than for those at the top. In particular, this diminishing returns hypothesis can explain why average life expectancy would be negatively related to income inequality when comparing societies with similar average incomes.

Adopting a more holistic view on health beyond mortality rates, we note that within the literature on socioeconomic inequality and public health, the relationship between inequalities and infectious diseases has received much less attention. Higher levels of income inequality were found to be associated with an increase in the incidence of chlamydia, gonorrhea and syphilis [37], as well as AIDS [23], thus supporting the view that greater income inequality correlates with worsened health

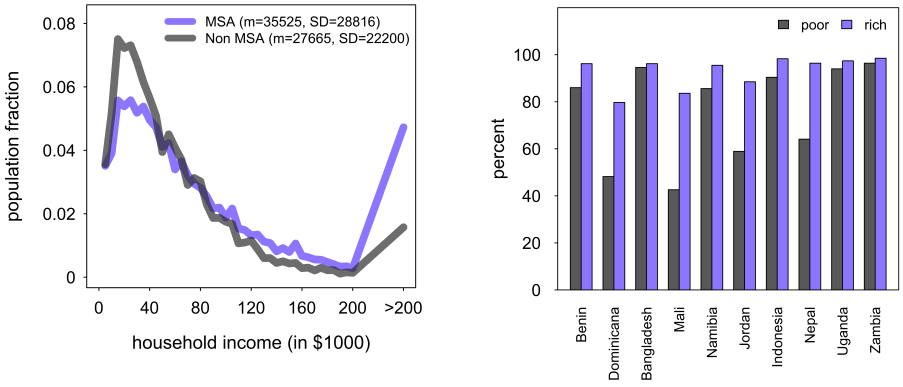

FIGURE 1. **(left)** Household Income distribution in MSA and non MSA areas of the U.S. in 2011. The mean (m) and standard deviation (SD) are computed excluding the fraction that makes more than $200,000. Even though average income in MSAs is larger, the income distribution in MSAs is broader (larger SD) than in non MSAs, suggesting larger income inequalities. Data Source: U.S. Census Bureau, Current Population Survey, 2012 Annual Social and Economic Supplement. **(right)** HIV/AIDS transmission dynamics knowledge in urban areas. In all represented countries, poorer residents within urban areas have less knowledge regarding the transmission of HIV. Data Source: World Health Organization.

outcomes. These association studies, however, do not provide a clear mechanistic explanation for how income inequalities affect the spread of infectious diseases.

Through the scope of a mathematical model, this paper aims to provide a more mechanistic understanding of the impact of socioeconomic inequalities on the dynamics of infectious diseases. As explained below, we focus on diseases that do not confer lasting immunity (such as certain sexually transmitted diseases) and we assume that the population can be divided into two groups that differ in their recovery rates due to differences in access to healthcare. We also address some of the consequences of relaxing these assumptions.

Epidemic model formulation. As noted above, it has been found that some sexually transmitted diseases, such as chlamydia, gonorrhea and syphilis, occur at higher rates in urban areas with greater levels of income inequality [37]. Because these diseases confer only temporary immunity upon recovery from infection, we will study the impact of healthcare access inequalities by modifying a Susceptible-Infected-Susceptible (SIS) epidemiological model. The SIS model has been widely used to study the dynamics of certain infectious diseases in both homogeneously [2, 6, 7, 24] and heterogeneously [8, 9, 22, 27] mixed populations, where following pathogen clearance from the host, due to treatment or immune response, an infectious individual recovers but is once again susceptible to infection.

In our framework, individuals belong to one of two groups based on their respective infectious periods. In this regard, we assume that the time from infection to treatment is significantly determined by individual socioeconomic aspects such

as income, education and access to healthcare services [18, 21]. In the model we postulate that the net outcome of all these factors can be represented by a single parameter, the recovery rate. Thus, how this parameter varies among individuals is a characterization of the health-related inequalities in the population. We assume that these two groups mix homogeneously in their shared geographic location (i.e., we are not dealing with a metapopulation model). Once individuals become infected, they recover at different per-capita rates γ_1 and γ_2, returning to their respective susceptible classes. We assume that individuals in group '1' recover at a faster rate, thus $\gamma_1 \geq \gamma_2$. Our main objective is to understand how the dynamics of the infectious disease are affected by variation in the recovery rates γ_1 and γ_2 between the two groups.

For the sake of clarity and simplicity of argument, for the moment we neglect differences in susceptibility, although we recognize that these also could influence the relationship between socioeconomic inequality and infectious disease [35]. In the discussion and in Appendix H we investigate the effects of having a population divided into two groups with different susceptibilities.

Mathematical model and the basic reproduction number. Consider a closed population of constant size N which is divided into two groups that differ in their access to healthcare. The first group represents a proportion f of the total population and its individuals have better healthcare access than those in the second group. In keeping with the SIS framework, we will assume that each individual is either susceptible or infected, and we let S_i and I_i represent the proportion of susceptible and infected individuals, respectively, of group i (where $i \in \{1, 2\}$). Thus, $S_1 + I_1 = f$ and $S_2 + I_2 = 1 - f$. Assuming that susceptible individuals in both groups are equally susceptible and are infected at a rate $\beta(I_1 + I_2)$, the SIS model can be completely specified by the following two equations,

$$\begin{aligned} \frac{dI_1}{dt} &= \beta(f - I_1)(I_1 + I_2) - \gamma_1 I_1, \\ \frac{dI_2}{dt} &= \beta[(1 - f) - I_2](I_1 + I_2) - \gamma_2 I_2, \end{aligned} \tag{1}$$

where the respective susceptible populations are given by $S_1 = f - I_1$ and $S_2 = 1 - f - I_2$.

The basic reproductive number, defined as the expected number of secondary infectious cases generated by a typical infectious case in an entirely susceptible population, is a key parameter in the analysis of infectious disease dynamics. In particular, it provides important insight into the following three issues: i) the potential for an infectious agent to start an outbreak, ii) the extent of transmission in the absence of control measures, and iii) our ability to deploy control measures to reduce a potential spread [28].

Following the Next Generation Matrix approach described in [42], the basic reproduction number is given by:

$$\mathcal{R}_0 = \beta \left(\frac{f}{\gamma_1} + \frac{1 - f}{\gamma_2} \right). \tag{2}$$

From Eq.(2) we can clearly see that the reproduction number has a contribution from the fast-recovering group and one from the slow-recovering group, each weighted by their respective representativeness in the population.

Conditions for the existence and stability of equilibria. Steady states of model (1) can be obtained by setting the derivatives in the left hand side equal to zero and then solving for I_1 and I_2. The model has both an infection-free equilibrium (IFE) $E_0 = (0, 0)$ and an endemic equilibrium $E^* = (I_1^*, I_2^*)'$, which will be determined below. The stability of the IFE is determined by the trace and determinant of the matrix of the linearized system at the IFE [41], and in Appendix B we prove the following proposition:

Proposition 1. *The infection-free equilibrium $E_0 = (0, 0)'$ is locally asymptotically stable if and only if $\mathcal{R}_0 < 1$.*

In addition, the endemic equilibria of system (1), namely I_1^* and I_2^*, are given by

$$I_1^* = \frac{f\lambda^*}{\lambda^* + \gamma_1} \qquad \text{and} \qquad I_2^* = \frac{(1-f)\lambda^*}{\lambda^* + \gamma_2}$$

where λ^* is the positive solution of the second-degree equation

$$F(\lambda^*) = {\lambda^*}^2 - \lambda^* Tr(\mathcal{L}) - \gamma_1\gamma_2\,(\mathcal{R}_0 - 1) = 0 \tag{3}$$

which is given by

$$\lambda^* = \frac{Tr(\mathcal{L}) + \sqrt{((Tr(\mathcal{L}))^2 + 4\gamma_1\gamma_2\,(\mathcal{R}_0 - 1)}}{2}, \tag{4}$$

with $\mathcal{L}$ being the matrix of the linearized system at the IFE:

$$\mathcal{L} = \begin{pmatrix} \beta f - \gamma_1 & \beta f \\ \beta(1-f) & \beta(1-f) - \gamma_2 \end{pmatrix}. \tag{5}$$

It is easy to check that, for $\mathcal{R}_0 < 1$, all coefficients of the quadratic polynomial (3) are positive. Thus, equation (3) has no positive solution for $\mathcal{R}_0 < 1$. If $\mathcal{R}_0 > 1$, then equation (3) has a unique positive solution. Consequently, model (1) has a unique endemic equilibrium for $\mathcal{R}_0 > 1$. We summarize these results in the following proposition

Proposition 2. *If $\mathcal{R}_0 > 1$, then model (1) has a unique endemic equilibrium $E^* = (I_1^*, I_2^*)'$ which is locally asymptotically stable whenever it exists.*

The stability analysis of the equilibrium E^* is deferred to Appendix C.

For future analyses, we need to state the following proposition which is straightforward to prove.

Proposition 3. *The quantity λ^*, as well as the proportions I_1^* and I_2^*, satisfy the following properties:*

1. *$\lambda^* = 0$ (and therefore, $I_1^* = 0$ and $I_2^* = 0$) if and only if $\mathcal{R}_0 = 1$,*
2. *I_1^* increases with λ^*, and*
3. *I_2^* increases with λ^*.*

Analysis in terms of the mean and the variance of recovery rates. In this section we describe how the dynamics of the SIS model depend on the variance in the recovery rates when the mean recovery rate is kept constant. Formally, the (weighted) mean (μ) and the variance (ν) of the recovery rates in this two-group population are given by

$$\mu = f\gamma_1 + (1-f)\gamma_2, \qquad \nu = f(\gamma_1 - \mu)^2 + (1-f)(\gamma_2 - \mu)^2.$$

Isolating γ_1 and γ_2 from these two expressions yields:

$$\gamma_1 = \mu + \sqrt{\frac{(1-f)\nu}{f}}, \qquad \gamma_2 = \mu - \sqrt{\frac{f\nu}{(1-f)}}. \tag{6}$$

In particular, we observe that for the inequality $\gamma_2 > 0$ to be satisfied, the variance must satisfy the inequality $\nu < \mu^2(1-f)/f := \nu^{max}$.

Reproduction number in terms of the mean and the variance. Substituting the expressions in (6) into $\mathcal{R}_0$ in (2) gives

$$\mathcal{R}_0 = \beta \left(\frac{f}{\mu + \sqrt{\frac{(1-f)\nu}{f}}} + \frac{1-f}{\mu - \sqrt{\frac{f\nu}{(1-f)}}} \right). \tag{7}$$

In particular, we would like to know how $\mathcal{R}_0$ varies with ν when f and μ are held constant, which we can do by calculating the partial derivative $\frac{\partial \mathcal{R}_0}{\partial \nu}$ [1]. In Appendix G we show that

$$\frac{\partial \mathcal{R}_0}{\partial \nu} > 0$$

for all biologically relevant values of μ and f. Hence, increasing the variance increases the reproductive number of the disease.

Similarly, we can determine the values of ν for which the infection will persist by studying the inequality $R_0(\nu) > 1$, which is equivalent to

$$F(\nu) := \nu + \frac{(1-2f)(\beta-\mu)}{\sqrt{f(1-f)}}\nu^{\frac{1}{2}} + \mu(\beta-\mu) > 0. \tag{8}$$

It is clear that if $\nu = 0$, the relation (8) holds if and only if $\mu < \beta$. However, if $\mu > \beta$, then $\mu(\beta-\mu) < 0$ and, therefore, irrespective of the sign of the coefficient of $\nu^{\frac{1}{2}}$, the inequality (8) holds if and only if $\nu > \nu_1$ where

$$\nu_1 \quad = \quad \left[\frac{(\mu-\beta)}{2\sqrt{f(1-f)}} \left(1 - 2f + \sqrt{1 + 4f(1-f)\frac{\beta}{\mu-\beta}} \right) \right]^2. \tag{9}$$

We summarize our results in the following proposition.

Proposition 4. *The basic reproduction number, as a function of the variance ν, is such that*

- $\mathcal{R}_0$ *always increases with* ν,
- $\mathcal{R}_0 > 1$ *if and only if either of the following is held*

$$\mu \quad < \quad \beta \quad \textit{or} \tag{10}$$

$$\mu \quad > \quad \beta \quad \textit{and} \quad \nu > \nu_1. \tag{11}$$

- $\mathcal{R}_0 = 1$ *only if* $\beta = \mu$ *or* $(\mu > \beta \quad \textit{and} \quad \nu = \nu_1)$

This result is illustrated in Figure 2, where we also see that when μ is small, increasing ν has a larger impact on $\mathcal{R}_0$. That is, the variance in recovery rates matters more when the average recovery of individuals is slow. Moreover, even when individuals recover fast enough on average as to make the quantity β/μ (the

[1] It is prudent to remark that the change in $\nu(\gamma_1, \gamma_2, f)$ in this partial derivative can only be due to changes in γ_1 and γ_2, not in f, given that f is held constant in the rest of the expression for $\mathcal{R}_0$.

standard way of quantifying the reproduction number) less than 1, the disease can still persist if there is sufficient heterogeneity in the population.

Figure 2 also suggests that the basic reproductive number will increase more rapidly with ν when the fraction f of individuals in the fast-recovering group is larger. Formally,

$$\frac{\partial(\partial\mathcal{R}_0(\nu,f)/\partial\nu)}{\partial f} > 0, \quad \forall f < f^{max} = \frac{\mu^2}{\nu+\mu^2}, \tag{12}$$

where f^{max} is the value of f over which $\gamma_2 < 0$; thus values of f larger than f^{max} are not relevant to our purposes. The expression (12) has been confirmed via numerical experiments. Moreover, it is clear from Figure 2 that for a given value of ν, if $f_1 > f_2$, then $\mathcal{R}_0(f_1) > \mathcal{R}_0(f_2)$, which seems counterintuitive at first sight. In fact, extensive numerical explorations suggest that, all else being equal, $\mathcal{R}_0$ increases with f. One way to make sense of this observation is by realizing that, if μ and γ_1 are held fixed, then γ_2 must decrease as f increases, meaning that those that recover at the slower rate are that much worse off. In other words, increasing f decreases γ_2 at a rate that offsets the benefits of having a larger fraction of the population recovering at a faster pace. Furthermore, increasing f augments the pool of fast-recovering susceptible individuals that can be infected multiple times by individuals with longer periods of infection; hence an increase in the expected number of new infections generated by each slow-recovering individual which results in the increase of $\mathcal{R}_0$.

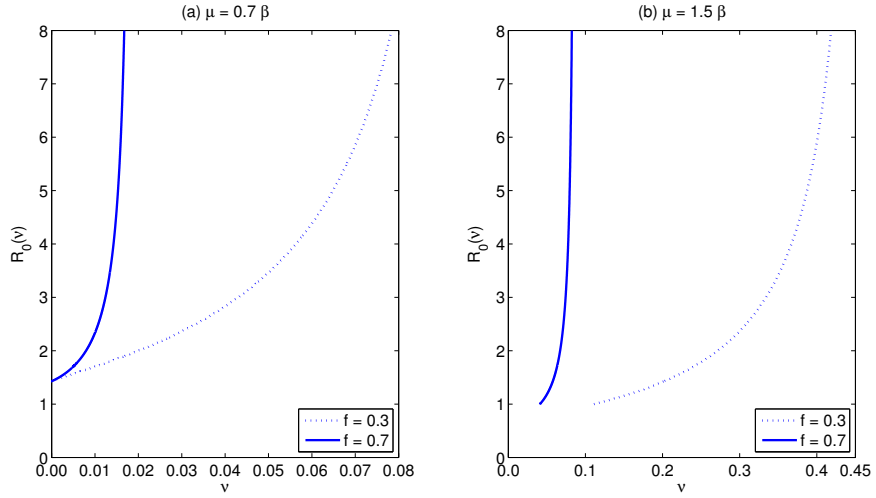

FIGURE 2. Reproduction number as a function of the variance ν, for different populations structures: $f = 0.3$ and $f = 0.7$. Part (a) shows the case $\mu < \beta$, while part (b) shows the case $\mu > \beta$, where $\beta = 0.3$. Note that in part (b), the variance has to be relatively large for the reproduction number to increase beyond 1. Notice also that $\mathcal{R}_0$ increases more steeply with ν for larger values of f. The graphs have vertical asymptotes for $\nu^{max} = \mu^2(1-f)/f$, at which point $\gamma_2 = 0$.

Prevalence in terms of the mean and the variance. The endemic prevalence $I_T^* = I_1^* + I_2^*$ as a function of the mean μ and the variance ν is given by

$$I_T^* = \frac{1}{2\beta}\left[\beta - 2\mu - \frac{(1-2f)}{\sqrt{f(1-f)}}\nu^{\frac{1}{2}} + \sqrt{\left(\beta + \frac{1}{\sqrt{f(1-f)}}\nu^{\frac{1}{2}}\right)^2 - \frac{4f\beta}{\sqrt{f(1-f)}}\nu^{\frac{1}{2}}}\right]. \tag{13}$$

To investigate the system in the limit of no heterogeneity, it is easy to check that

$$\lim_{\nu\to 0^+} I_T^*(\nu) = \left(1 - \frac{\mu}{\beta}\right) \tag{14}$$

which is positive if and only if $\beta > \mu$. Hence, in case $\mu > \beta$, the proportion I_T^* is negative for values of ν in the neighborhood of $\nu = 0$ (in fact, $I_T^* < 0$ for all values of ν less than ν_1). In further investigating the behavior of $I_T^*(\nu)$ near the no-heterogeneity limit, we find that

$$\lim_{\nu\to 0^+} \frac{\partial I_T^*}{\partial \nu} = \frac{1}{\beta^2} > 0. \tag{15}$$

This inequality implies that the endemic prevalence $I_T^*(\nu)$ increases initially with the increase of the variance ν.

It is easy to check that

$$I_T^*(\nu^{max}) = \frac{1}{2\beta}\left[\beta - \frac{\mu}{f} + \sqrt{\left(\beta - \frac{\mu}{f}\right)^2 + 4(1-f)\beta\frac{\mu}{f}}\right] > 0. \tag{16}$$

Moreover, $I_T^* = 0$ if and only if $R_0 = 1$ (and by proposition 4) if and only if $\beta = \mu$ or ($\mu > \beta$ and $\nu = \nu_1$). Also, from the second item in proposition 3 and expression (4) it can be concluded that I_T^* increases with R_0, which in turn, by proposition 4, increases with ν. Thus, I_T^* always increases with ν. Figure 3 shows this behavior for different values of model parameters. We collect the above results to state the following proposition that shows the qualitative behavior of the prevalence of infection at equilibrium as a function of ν.

Proposition 5. *The qualitative behavior of the prevalence $I_T^*(\nu)$ has two cases:*

1. **Case 1:** *$\mu \leq \beta$. In this case, $I_T^*(\nu = 0) > 0$ and, therefore, $I_T^*(\nu)$ is always increasing until reaching its maximum at $\nu = \nu^{max}$ (see Figure 3(a) & (b)).*
2. **Case 2:** *$\mu > \beta$. Here, $\mathcal{R}_0(\nu = 0) < 1, I_T^*(\nu = 0) < 0$ and therefore I_T^* is defined only for $\nu \geq \nu_1$, with $I_T^*(\nu = \nu_1) = 0$. In this case I_T^* increases whenever it is defined, reaching its maximum at $\nu = \nu^{max}$ (see Figure 3(c) & (d)).*

Analysis in populations with multiple groups with different recovery rates. In the previous section we assumed that the population was subdivided into only two groups. More generally, individuals can be part of K "recovery" groups. In that case, one would need $K-1$ fractions f_i, $i = \{1, K-1\}$, to fully determine the "inequality" structure of the population. Extending our analysis to the more general case where the population is divided into K groups, each representing a fraction f_k of the population and with recovery rates γ_k with $k \in \{1, 2, 3...K\}$, it can be shown using the Next Generation Matrix method [42] that the basic reproduction

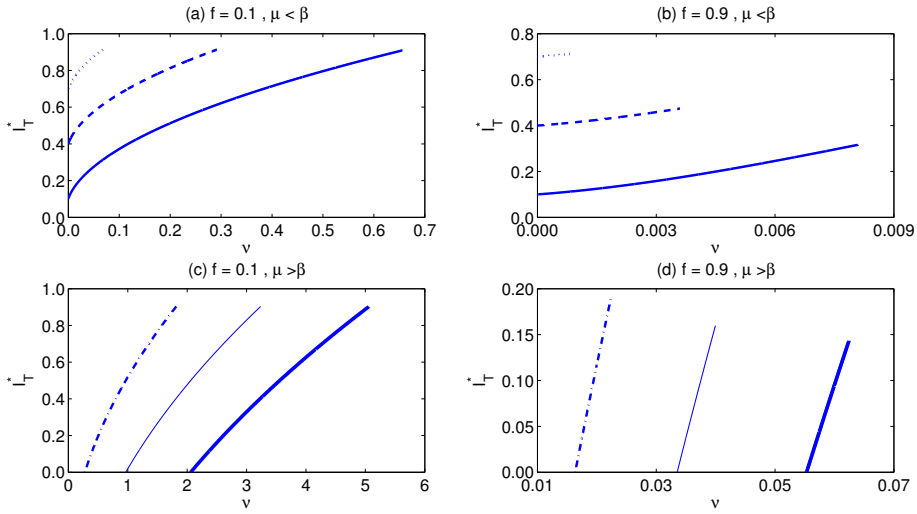

FIGURE 3. The prevalence I_T^* as a function of the variance, for different values of f and μ, as explained in the heads of each subfigure. Parts (a) and (b) are drawn with $\mu = 0.3\beta$ (dotted curves), $\mu = 0.6\beta$ (broken curves) and $\mu = 0.9\beta$ (solid curves). However, parts (c) and (d) are done with values of $\mu = 1.5\beta$ (dashed-dotted curves), $\mu = 2\beta$ (thin-solid curves) and $\mu = 2.5\beta$ (heavy-solid curves).

number is given by

$$\mathcal{R}_0 = \beta \sum_{k=1}^{K} \frac{f_k}{\gamma_k}.$$

In other words, we can write the basic reproductive number as $\mathcal{R}_0 = \beta/m_h$, where $m_h = \left(\sum_k \frac{f_k}{\gamma_k}\right)^{-1}$ is the weighted harmonic mean of the recovery rates over the different groups making up the population. In contrast, the arithmetic mean would be given by $m_a = \sum_k f_k \gamma_k$. It is known that the harmonic mean is less than the arithmetic mean, i.e., $m_h < m_a$, thus $\mathcal{R}_0 = \beta/m_h > \beta/m_a$.

Let us compare two cases: i) the limiting case where the population is composed of only one group of individuals with recovery rate given by m_a, and ii) the population is split into K groups based on their recovery rates, while preserving the mean recovery rate. In case i) the reproduction number would be given by β/m_a, whereas the second scenario leads to a reproduction number equal to β/m_h, with $\beta/m_a < \beta/m_h$ as we have just shown. Thus, we can conclude that a disease has less potential to spread in a homogeneous population than in a heterogeneous with the same mean recovery rate[2]. In other words, recovery-rate heterogeneity in the population increases the transmission potential of a disease.

[2]In this paper we equate the term "heterogeneity in the population" to the variance of the recovery rates in the population. We note that this equivalency can be ambiguous in certain situations, such as in the case where the recovery rates in the population follow "fat-tail" distributions, which can feature large variances even though most recovery rates are concentrated around a given value, and can therefore be effectively characterized as a homogeneous population.

Analysis via agent-based model simulations. Here we build on the idea of multiple groups with different healthcare access. We take an agent-based approach where instead of having two groups of individuals characterized by two different recovery rates, each individual is assigned a recovery rate. As before, we aim to better understand how recovery rate heterogeneity affects disease prevalence in the population.

Other models have already shown the importance of heterogeneity among individuals [31, 15, 20, 35], and the implications for disease dynamics due to the inclusion of more realistic infectious period distribution [25, 29, 30, 44, 28]. For example, the authors in [30] used a Susceptible-Infected-Recovered (SIR) type framework and found that less dispersed infectious periods destabilize the dynamics, leading more often to extinction or to larger stochastic fluctuations around the endemic equilibrium. In the context of SARS, [28] showed that if there is large variation in the number of secondary cases generated by each index case, the probability of a large epidemic is lessened as compared to the cases with less variation.

The model we present here conforms to the SIS type model we have been using thus far. Susceptible individuals are infected at a rate proportional to the frequency of interactions with infected individuals, and the transmission rate, β. In contrast to the two-group approach presented before, the recovery rates of each individual in this model are sampled from distributions with different properties (e.g., variance), allowing us to assess how these properties affect disease outcome.

By assuming that the transition processes from one class to another is a homogeneous Poisson process, the conditional probability that an individual susceptible at time t becomes infected between time t and $t + dt$, say $\mathbb{P}_I(t)$, is given by

$$\mathbb{P}_I(t) = 1 - \exp(-\beta I(t)dt/N) + o(dt), \tag{17}$$

where the other parameters in the transition rate are $I(t)$, the number of infected at time t, and the size of the population, N.

When infected, individuals recover at different rates, moving back to the susceptible class. We model the recovery rate as a random variable with a Beta distribution kernel (see Appendix I for details). Using the Beta distribution as a kernel allows for the shape of this distribution to be considered a descriptive proxy for the structure of inequalities in the population. Different inequality profiles– that is, distribution profiles– can be easily obtained by calibrating the parameters in the distribution, making this theoretical framework quite flexible to test the effects of different inequality profiles on epidemic outcomes. More specifically, we focus on symmetric recovery rate distributions with fixed means, and test the effects of changing the variance of the distribution.

In the simulations, once a recovery rate, namely γ_i, has been assigned to the ith agent, the duration of each infection suffered by this agent is exponentially distributed with mean $1/\gamma_i$. It is noteworthy that the distribution of infectious periods does not necessarily share the same symmetry properties as that of the recovery rates. In fact, when the recovery rates are symmetrically distributed, the distribution of infectious periods tend to be skewed to the right.

In addition to exploring the role of the variance on disease prevalence, we investigated the role of the mean recovery rate as well as pathogen transmissibility. For each run, the prevalence was computed as the mean of the prevalence values over the last 100 time steps conditional on non extinction. For each parameter value, we plot the mean of prevalences over 20 simulations, along with the standard

errors, versus the variance of the corresponding recovery rates distributions. For more details regarding the simulation set up see Appendix I.

In line with results thus far, Figure 4 shows that the prevalence increases along with the variance of the recovery rates. Moreover, the rate of increase is different for different transmission rates and different mean recovery rates. The effect of the variance of the recovery rates on the prevalence is larger for less transmissible diseases. Additionally, we find that the effect of the variance on the prevalence is larger when individuals recover faster on average.

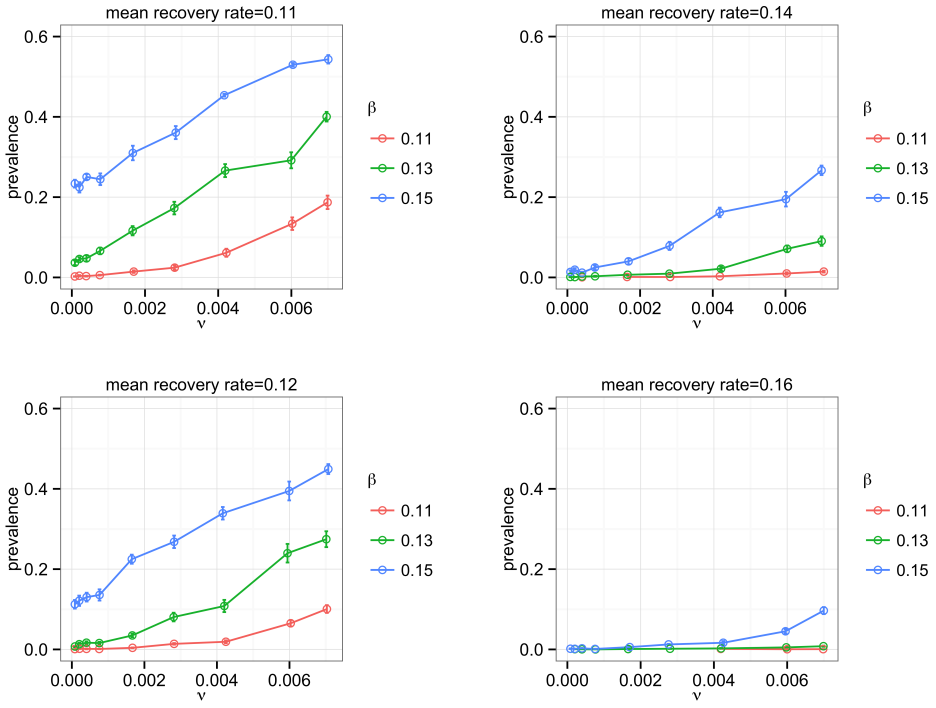

FIGURE 4. Mean and standard error (bars) of the infection prevalence (fraction) versus variance of the recovery rates for different values of the mean recovery rate and the transmission rate.

Discussion. In a world where socioeconomic inequalities are increasing, our understanding of the role of inequalities in epidemic outcomes is paramount. As a first step to investigate this issue, we model a scenario where a homogeneously mixed population is divided into two groups of people with different recovery rates (as a proxy for healthcare access). With this modeling approach, we demonstrate that increasing inequalities can have important effects on the spreading potential (i.e., epidemic risk and size) of certain pathogens, such as curable STDs. Specifically, both $\mathcal{R}_0$ and the endemic prevalence are shown to always increase with the variance of recovery rates (i.e., inequalities) whenever the mean recovery rate is held constant. Moreover, for large values of the mean recovery rate, the disease can still persist when the variance is sufficiently large.

From our analyses we can also infer that, for a fixed mean recovery rate, increasing the fraction of the population that recovers faster, leads to an increase in the transmission potential of the disease. This insight suggests that a public health intervention that aims at increasing the fraction of individuals with better healthcare access at the expense of those with less access could be worsening the epidemiological situation. Put differently, interventions designed to quell the spread of infectious diseases should aim to both decrease inequality and improve the overall access to healthcare.

In Appendix A, these effects are analyzed in terms of the unweighted mean of recovery rates and difference in recovery rates between the two groups. In contrast to the results reported above, focusing on the unweighted mean and difference depicts a more complex picture, with the dynamics of epidemic spread depending more closely on the structure of the population. Importantly, the contrasting nature of the conclusions derived from these two different approaches underscores the importance of focusing on the right quantities. We consider that focusing on the mean and variance, rather than the unweighted mean and difference of recovery rates, is the appropriate way to study the effects of inequalities on epidemic outcomes.

Extending our analyses to the more general case where the population is composed of K different groups with different recovery rates, we show that the reproduction number is always greater in the presence of a heterogeneous population than in the case where there is no heterogeneity in recovery rates, if the mean recovery rate is preserved. Through this analysis we can also conclude that if we were to quantify the overall recovery rate of the population using the arithmetic mean, we would be underestimating the reproduction number, underscoring the importance of properly accounting for population heterogeneity.

Building upon this approach, we present a stochastic agent-based model in which each individual in the population is assigned a recovery rate. In line with the results reported thus far, this agent-based model reveals that the prevalence increases with the variance of the distribution of recovery rates. In addition, as noted before based on the two-group deterministic model, as the mean recovery rate increases, the disease can only persist when the variance is also large. Moreover, the prevalence is more sensitive to changes in recovery-rate variance for diseases with lower spreading potential.

This study has a number of limitations. The socioeconomic context of individuals not only affects the speed of recovery, but it is also tied in to the likelihood of becoming infected in the first place, which would be reflected in the transmission rate β. However, for the sake of clarity, we have assumed that social inequalities only result in heterogeneities of recovery rates. A more realistic version of the model would add heterogeneity of transmission/susceptibility. To obtain a deeper understanding of the linkage between social inequality and public health outcomes, in Appendix H we generalize model (1) to include a dichotomous susceptible population by assuming that individuals in the group with better healthcare facilities are also less susceptible to infection. The analyses of this extended model reveals that increasing the variance in susceptibility diminishes the effects of increased variance in recovery. Put differently, the effects of having less-susceptible individuals counterbalances the effects of a slow recovering infected population.

One key assumption of this deterministic approach, also present in the stochastic model, is that recovery times are exponentially distributed. In fact, the stochastic model gave us insight into a factor possibly contributing to the observation that

higher prevalence of disease follows larger variance of recovery rates. Even though the recovery rates were symmetrically distributed, the recovery times were skewed to the right, as expected given the skewness of the exponential distribution. Furthermore, as the variance of the recovery rates decreases so does the variance of the recovery times, but also the mean of the recovery times decreases, with these faster recovery times leading to lower disease prevalence. This could partly account for the relation we observe between variance and prevalence. Consequently, we believe this issue should be further explored by relaxing the exponentially distributed times assumption.

Furthermore, we have assumed that immunity is fleeting after recovery, which is not always realistic since many infections confer at least some temporal immunity after recovery. To relax this model assumption, we could also consider an susceptible-infected-removed-susceptible (SIRS) framework, instead of SIS, where individuals remain immune to the disease for a certain period of time (more appropriate for diseases such as influenza). In this case we hypothesize that if the rate at which individuals lose immunity (rate of transit from R to S) is the same for all individuals, then the results we show here should hold at least qualitatively.

The SIS framework in this paper is a simple model of an endemic disease. Hence, the conclusions derived with this model are not necessarily applicable for models of single-wave outbreaks (e.g., susceptible-infected-removed (SIR) type models), due in part to the absence of an endemic state in the latter models. We expect, however, that health-care access inequalities may also play an important role in the growth rate and final size of single epidemic outbreaks.

Finally, an important aspect that has been overlooked so far is the mixing between the two types of populations. We have assumed that both populations mix homogeneously, but this is not likely to be the case in reality. In reality, we expect that individuals interact only with certain others and, moreover, individuals are more likely to interact with other of the same socioeconomic status (homophily) [36, 5]. For example, in the case of patterns of sexual mixing, the evidence shows that relationships are more common between persons of the same ethnicity [16, 17]. Thus a clear way to relax our model assumptions is to assume that the levels of mixing with individuals of the other group is smaller than with individuals of the same group. This new assumptions could change the conclusions reached in this study, and hence we expect that this study will motivate further investigation of the issue of inequalities and epidemic outcomes.

Overall, these insights shed light on the interplay between health-care access inequalities and the risk and endemic burden of epidemics. It shows that how the population is structured in terms of its access to healthcare services plays a crucial role in the pathogen's spreading potential. In particular, increasing inequalities often worsen epidemic outcomes. This conclusion is in agreement with the empirical evidence suggesting that larger levels of socioeconomic inequalities are often associated with worsened health outcomes; thus our model offers a mechanistic explanation for these empirical patterns.

Acknowledgments. The authors would like to thank the reviewers for helpful comments on the manuscript.

Appendices.

Appendix A: Analysis in terms of unweighted mean and difference of recovery rates. In this section we take a slightly different approach by focusing on different quantities to study the role of inequalities in disease dynamics. Arguably, the simplest setting in which to assess the epidemic impact of inequality in recovery rates is by assuming the average of the rates to be constant and investigating the role of the gap between the two groups in healthcare accessibilities.

Let the levels of inequality between the two populations be represented by two parameters related to the recovery rates: the unweighted mean $\mu_\gamma = (\gamma_1 + \gamma_2)/2$ and the difference $\Delta_\gamma = \gamma_1 - \gamma_2 > 0$. This formulation implies that the larger the value of Δ_γ is, the larger the extent of inequalities is, with $\Delta_\gamma = 0$ signifying complete equality between the groups.

Since we intend to focus on the effect of inequality on disease outcome (i.e., $\mathcal{R}_0$ and prevalence), we fix the mean μ_γ and redefine recovery rates as follows

$$\gamma_1 = \mu_\gamma + \frac{\Delta_\gamma}{2}, \quad \gamma_2 = \mu_\gamma - \frac{\Delta_\gamma}{2} \tag{18}$$

where it is required that $\mu_\gamma \geq \Delta_\gamma/2$ such that $\gamma_2 \geq 0$. Thus, $\Delta_\gamma \in [0, 2\mu_\gamma)$.

Impact of recovery rate inequalities on the value of $\mathcal{R}_0$. The expression of $\mathcal{R}_0$ can provide useful insights into the role of inequalities in recovery rates and the persistence of disease. Using the new terms in (18), the reproduction number $\mathcal{R}_0$ can be rewritten as

$$\mathcal{R}_0 = \beta \left[\frac{f}{\mu_\gamma + \Delta_\gamma/2} + \frac{1-f}{\mu_\gamma - \Delta_\gamma/2} \right] \tag{19}$$

For the rest of this section we will slightly change the nomenclature from $\Delta_\gamma/2$ to simply Δ. Let us first analyze the case $f = 0.5$, that is, when exactly half the population recovers faster than the other half. It is easy to show that $\mathcal{R}_0(f = 0.5) = \beta\mu_\gamma/(\mu_\gamma^2 - \Delta^2)$, and since $\mu_\gamma > \Delta$, increasing Δ also increases the reproduction number. In other words, when the population is divided equally between those that recover faster and those that do so slowly, increasing the levels of recovery-rate inequalities also increases the transmission potential of the pathogen, leading in turn to larger endemic disease levels.

For the more general case when $f \in [0, 1]$, we take partial derivatives of $\mathcal{R}_0$ with respect to Δ. This derivative is positive if either of the following two conditions holds (see Appendix D for details)

$$f \leq \frac{1}{2} \quad \text{or} \tag{20}$$

$$f > \frac{1}{2} \quad \text{and} \quad \Delta > \Delta_2 \tag{21}$$

where

$$\Delta_2 = \frac{\sqrt{f} - \sqrt{1-f}}{\sqrt{f} + \sqrt{1-f}} \mu_\gamma. \tag{22}$$

Condition (20) says that if the fraction of population that has proper access to healthcare facilities is less than half, then the basic reproduction number increases with the increase of the difference Δ. However, condition (21) says that if that proportion is more than half then $\mathcal{R}_0$ decreases initially with Δ until it reaches a

minimum value $\mathcal{R}_0^*$ at $\Delta = \Delta_2$, and then it starts to increase until reaching its possible maximum at $\Delta = \mu_\gamma$, where

$$\mathcal{R}_0^* = \mathcal{R}_0(\Delta_2) = \frac{\beta}{2\mu_\gamma}\left(\sqrt{f} + \sqrt{1-f}\right)^2 \leq \frac{\beta}{\mu_\gamma}. \tag{23}$$

We also investigated the space of parameters for which the infection persists by studying the possible parameter values for which the inequality $\mathcal{R}_0 > 1$ holds (see Appendix E for details). Figure 5 and Table 1 summarize the qualitative behavior of the basic reproduction number in the different parameters' domain spaces. Interestingly, notice that when $\mu_\gamma > \beta$ (for which the reproduction number would be less than one if we were to compute it using the unweighted mean μ_γ) the infection can persist due to heterogeneities in healthcare accessibilities.

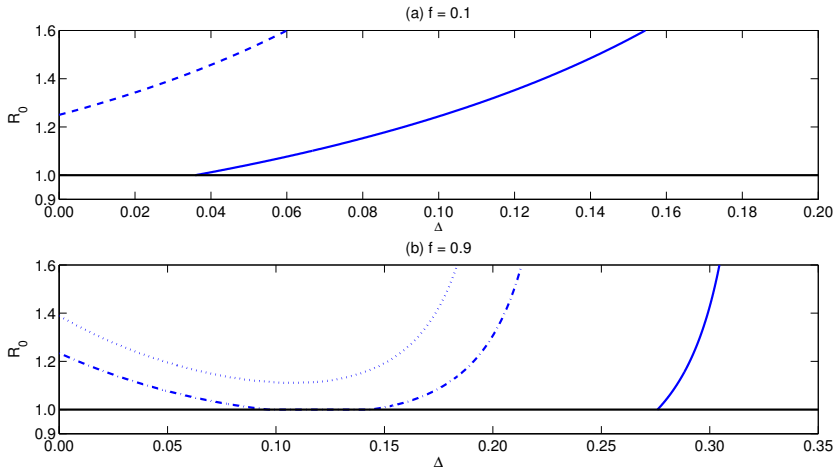

FIGURE 5. Reproduction number as a function of recovery rate difference Δ, for transmission rate $\beta = 0.3$ and different values of f and mean of recovery rates μ_γ. Part (a) shows the case of $f = 0.1$ and $\mu_\gamma = 0.8\beta$ (broken curve), $\mu_\gamma = 1.1\beta$ (solid curve). Part (b) shows the case of $f = 0.9$ and $\mu_\gamma = 0.9\mu_\gamma^*$ (dotted curve); $\mu_\gamma = \mu_\gamma^* + 0.05(\beta - \mu_\gamma^*)$ (dashed-dotted curve); $\mu_\gamma = 1.1\beta$ (solid curve). Here $\mu_\gamma^* = \frac{\beta}{2}\left(\sqrt{f} + \sqrt{1-f}\right)^2$.

Through this simple approach, we would also like to understand the role of the mean of the recovery rates, namely μ_γ, in the impact of inequalities on epidemic persistence and size. In other words, we would like to know when do inequalities matter most?

Expression (22) indicates that, when $\Delta_2 > 0$, as μ_γ increases so does Δ_2, thus enlarging the range $(0, \Delta_2)$ in which the reproduction number decreases with larger inequalities. Figure 6 also shows that the smaller μ_γ is, the more the more sensitive $\mathcal{R}_0$ is to changes in Δ. In other words, the slower individuals recover, on average, the more variations in inequalities affect the transmission potential of the disease. As noticed before, when the majority recovers slowly ($f < 0.5$) increasing inequalities leads to higher reproduction numbers, whereas if the majority recovers at a larger rate ($f > 0.5$), the effect of increasing inequalities depends on the magnitude of

TABLE 1. Parameters' domain space for which $R_0 > 1$ and notes on the qualitative behavior of R_0, see Figure 5. See Appendix E for the definitions of $\tilde{\Delta}_1$ and $\tilde{\Delta}_2$.

f	μ_γ	Domain of Δ	Notes on the qualitative behavior of $\mathcal{R}_0(\Delta)$
$f \leq \frac{1}{2}$	$\mu_\gamma < \beta$	$--$	Increasing
	$\mu_\gamma > \beta$	$\Delta < \tilde{\Delta}_2$	less than 1 and the infection dies out
		$\Delta > \tilde{\Delta}_2$	Increasing
$f > \frac{1}{2}$	$\mu_\gamma < \frac{\beta}{2}\left(\sqrt{f} + \sqrt{1-f}\right)^2$	$\Delta < \Delta_2$	Decreasing
		$\Delta > \Delta_2$	Increasing
	$\frac{\beta}{2}\left(\sqrt{f} + \sqrt{1-f}\right)^2 < \mu_\gamma < \beta$	$\Delta < \tilde{\Delta}_1$	Decreasing with $R_0(\Delta = \tilde{\Delta}_1) = 1$
		$\tilde{\Delta}_1 < \Delta < \tilde{\Delta}_2$	less than 1 and the infection dies out
		$\Delta > \tilde{\Delta}_2$	Increasing with $R_0(\Delta = \tilde{\Delta}_2) = 1$
	$\mu_\gamma > \beta$	$\Delta > \tilde{\Delta}_2$	Increasing

the inequalities themselves: increasing inequalities when these are relatively low will keep decreasing them, but if inequalities are relatively large, further increasing them can in fact improve the transmission potential of the pathogen.

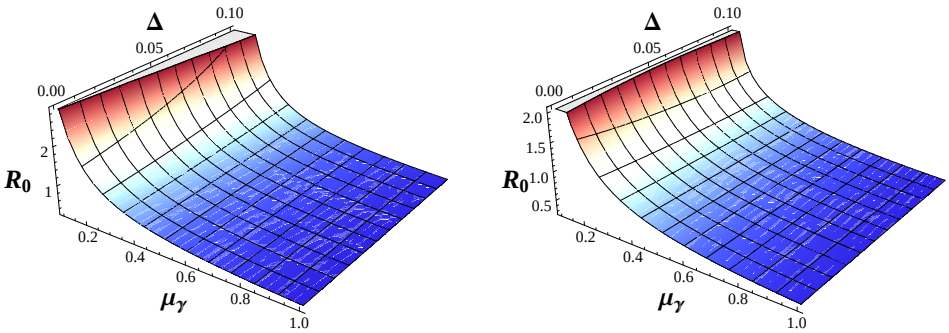

FIGURE 6. Reproduction number as a function of recovery rate difference Δ and mean of recovery rates μ_γ. Other parameters: $\beta = 0.3$ and $f = 0.1$ (left) and $f = 0.9$ (right).

Impact of recovery rate inequalities on the endemic prevalence of infection. In this section we study the role of recovery rate inequality on prevalence levels. The total fraction infected at the endemic equilibrium, given by $I_T^* = I_1^* + I_2^*$, can be written in terms of μ_γ and Δ as

$$I_T^* = \frac{1}{2\beta}\{\beta - 2\mu_\gamma + \sqrt{(\beta + 2\Delta)^2 - 8f\beta\Delta}\}. \tag{24}$$

In Appendix F we show that for certain parameter conditions, the prevalence I_T^* i) increases with Δ until reaching a maximum at $\Delta = \mu_\gamma$; or ii) decreases initially until reaching a minimum at some value of Δ (say Δ^*) and then increases again to reach its maximum at $\Delta = \mu_\gamma$; or iii) decreases initially until reaching zero at $\Delta = \tilde{\Delta}_1$, and if Δ is further increased, then the infection starts to persist again at $\Delta = \tilde{\Delta}_2$ and continue to increase until reaching its maximum at $\Delta = \mu_\gamma$.

Table 2 and Figure 7 summarize the qualitative behavior in these different cases.

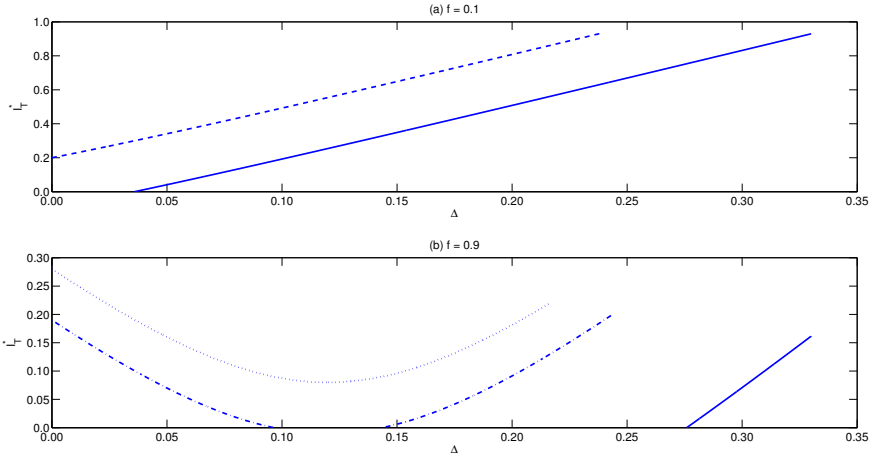

FIGURE 7. Endemic levels as a function of recovery rate difference Δ, for transmission rate $\beta = 0.3$ and different values of f and mean of recovery rates μ_γ. Part (a) shows the case of $f = 0.1$ and $\mu_\gamma = 0.8\beta$ (broken curve), $\mu_\gamma = 1.1\beta$ (solid curve). Part (b) shows the case of $f = 0.9$ and $\mu_\gamma = 0.9\mu_\gamma^*$ (dotted curve); $\mu_\gamma = \mu_\gamma^* + 0.05(\beta - \mu_\gamma^*)$ (dashed-dotted curve); $\mu_\gamma = 1.1\beta$ (solid curve). Here $\mu_\gamma^* = \frac{\beta}{2}\left(\sqrt{f} + \sqrt{1-f}\right)^2$.

Through this analysis we find, in contrast to the previous findings, that the effects of inequalities can be complex and context (parameter) dependent when focusing on the difference between recovery rates rather than the variance (see Appendix A for detailed analyses). In fact, Figures 5 and 7 illustrate that when the minority of individuals have proper access to healthcare services ($f < 1/2$), the reproduction number $\mathcal{R}_0$ increases with recovery rates difference (i.e., inequalities) when the average recovery rates are small (compared to the transmission rate), or when the average recovery rates are relatively large and inequalities are also large. In contrast, when the majority of them has proper access to healthcare services ($f > 1/2$), $\mathcal{R}_0$ decreases with inequalities when these and the average recovery rates are relatively small, whereas it increases with inequalities when these are large. The analysis

TABLE 2. Impact of changing the relevant parameters on the qualitative behavior of I_T^* as a function of recovery rate difference Δ, transmission rate β population structure f and mean of recovery rates μ_γ.

f	μ_γ	Domain of Δ	Notes on the qualitative behavior of $I_T^*(\Delta)$
$f \leq \frac{1}{2}$	$\mu_\gamma < \beta$	$--$	Increasing, where $I_T^*(\Delta = 0) > 0$
	$\mu_\gamma > \beta$	$\Delta < \tilde{\Delta}_2$	$I_T^* < 0$ and the infection dies out
		$\Delta > \tilde{\Delta}_2$	Increasing, where $I_T^*(\Delta = 0) < 0$ and $I_T^*(\Delta = \tilde{\Delta}_2) = 0$
$f > \frac{1}{2}$	$\mu_\gamma < \frac{\beta}{2}\left(\sqrt{f} + \sqrt{1-f}\right)^2$	$\Delta < \Delta_2$	Decreasing, with $I_T^*(\Delta_2) > 0$
		$\Delta > \Delta_2$	Increasing
	$\frac{\beta}{2}\left(\sqrt{f} + \sqrt{1-f}\right)^2 < \mu_\gamma < \beta$	$\Delta < \tilde{\Delta}_1$	Decreasing, with $I_T^*(\tilde{\Delta}_1) = 0$
		$\tilde{\Delta}_1 < \Delta < \tilde{\Delta}_2$	$I_T^*(\Delta) < 0$ and the infection dies out
		$\Delta > \tilde{\Delta}_2$	Increasing, with $I_T^*(\tilde{\Delta}_2) = 0$
	$\mu_\gamma > \beta$	$\Delta > \tilde{\Delta}_2$	Increasing, with $I_T^*(\tilde{\Delta}_2) = 0$

shows that the total fraction of infected individuals at the endemic equilibrium, I_T^*, follows a similar behavior, although it is important to notice that when average recovery rates are relatively large, it has no biological significance, since I_T^* is less than zero in those cases.

We note that there is no clear biologically meaningful connection between the unweighted mean (μ_γ) or difference (Δ) and the population dynamics. Moreover, the contrasting nature of the conclusions derived from the two different approaches underscores the importance of focusing on the right quantities. We consider that in this case, focusing on the mean and variance (as in the main text), rather than the unweighted mean and difference, of recovery rates is the appropriate way to study the effects of inequalities on epidemic outcomes. It is not only a more generalizable approach, but it is also the most sound from a mathematical perspective as it properly describes the inequalities in the population.

Appendix B: Stability of the infection free equilibrium E_0: The stability of the IFE can be characterized by the trace and determinant of the matrix of the linearized system at the IFE [41],

$$\mathcal{L} = \begin{pmatrix} \beta f - \gamma_1 & \beta f \\ \beta(1-f) & \beta(1-f) - \gamma_2 \end{pmatrix} \tag{25}$$

with trace and determinant given by

$$Tr(\mathcal{L}) = \beta - \gamma_1 - \gamma_2 \qquad \text{and} \qquad Det(\mathcal{L}) = -\beta(1-f)\gamma_1 - \beta f\gamma_2 + \gamma_1\gamma_2. \tag{26}$$

For the IFE to be locally stable, the trace has to be negative and the determinant has to be positive. These two conditions yield

$$Tr(\mathcal{L}) < 0 \implies \frac{\beta}{\gamma_1+\gamma_2} < 1 \qquad Det(\mathcal{L}) > 0 \implies \mathcal{R}_0 < 1. \tag{27}$$

It can be shown that, if $f \in [0,1]$, then $\mathcal{R}_0 > \frac{\beta}{\gamma_1+\gamma_2}$. Thus, if $\mathcal{R}_0 < 1 \implies Tr(\mathcal{L}) < 0$. Hence, we conclude that the IFE is locally asymptotically stable when $\mathcal{R}_0 < 1$.

Appendix C: Stability of the endemic equilibrium E^*: To establish the local stability of the endemic equilibrium we find the Jacobian matrix

$$J = \begin{pmatrix} \beta(f - I_1) - (\lambda^* + \gamma_1) & \beta(f - I_1) \\ \beta[(1-f) - I_2] & \beta[(1-f) - I_2] - (\lambda^* + \gamma_2) \end{pmatrix}. \tag{28}$$

At equilibrium, we have

$$f - I_1 = \frac{f\gamma_1}{(\lambda^* + \gamma_1)}, \qquad (1-f) - I_2 = \frac{(1-f)\gamma_2}{(\lambda^* + \gamma_2)} \tag{29}$$

and

$$(\lambda^* + \gamma_1)(\lambda^* + \gamma_2) = \beta[f(\lambda^* + \gamma_2) + (1-f)(\lambda^* + \gamma_1)] \tag{30}$$

The relation (30) implies that

$$\frac{\beta f(\lambda^* + \gamma_2)}{\lambda^* + \gamma_1} = \lambda^* + \gamma_2 - (1-f)\beta, \quad \text{and} \quad \frac{\beta(1-f)(\lambda^* + \gamma_1)}{\lambda^* + \gamma_2} = \lambda^* + \gamma_1 - f\beta \tag{31}$$

Using (29), (30), (31) in (28), we get

$$\begin{aligned} det(J) &= (\lambda^* + \gamma_1)(\lambda^* + \gamma_2) - \gamma_1(\lambda^* + \gamma_2) - \gamma_2(\lambda^* + \gamma_1) + \beta[(1-f)\gamma_1 + f\gamma_2] \\ &= \lambda^{*2} - [\gamma_1\gamma_2 - \beta(f\gamma_2 + (1-f)\gamma_1)] \\ &= \lambda^*[2\lambda^* + (\gamma_1 + \gamma_2 - \beta)] = \lambda^*[2\lambda^* - Tr(\mathcal{L})] \\ &= \lambda^*\sqrt{((Tr(\mathcal{L}))^2 + 4\gamma_1\gamma_2\,(\mathcal{R}_0 - 1)} > 0 \end{aligned}$$

and

$$\begin{aligned} Tr(J) &= \beta - (\gamma_1 + \gamma_2) - 3\lambda^* = Tr(\mathcal{L}) - 3\lambda^* \\ &= 2\lambda^* - \sqrt{((Tr(\mathcal{L}))^2 + 4\gamma_1\gamma_2\,(\mathcal{R}_0 - 1)} - 3\lambda^* \\ &= -\{\lambda^* + \sqrt{((Tr(\mathcal{L}))^2 + 4\gamma_1\gamma_2\,(\mathcal{R}_0 - 1)}\} < 0. \end{aligned}$$

Thus, the endemic equilibrium $E^* = (I_1^*, I_2^*)'$ is locally asymptotically stable whenever it exists.

Appendix D: Derivative of $\mathcal{R}_0$ with respect to Δ. We take partial derivatives of $\mathcal{R}_0$ with respect to Δ, yielding

$$\begin{aligned}\frac{\partial \mathcal{R}_0}{\partial \Delta} &= \beta\left(\frac{1-f}{(\mu_\gamma-\Delta)^2}-\frac{f}{(\mu_\gamma+\Delta)^2}\right). &(32)\\ &= \frac{\beta}{(\mu_\gamma^2-\Delta^2)^2}[(1-f)(\mu_\gamma+\Delta)^2-f(\mu_\gamma-\Delta)^2] \\ &= \frac{\beta\sqrt{f}[\sqrt{1-f}(\mu_\gamma+\Delta)+\sqrt{f}(\mu_\gamma-\Delta)]}{(\mu_\gamma^2-\Delta^2)^2}\times &(33)\\ &\quad \left[\left(-1+\sqrt{\frac{1}{f}-1}\right)\mu_\gamma+\left(1+\sqrt{\frac{1}{f}-1}\right)\Delta\right].\end{aligned}$$

Thus, the sign of $\partial\mathcal{R}_0/\partial\Delta$ depends mainly on the sign of the expression

$$\left[\left(-1+\sqrt{\frac{1}{f}-1}\right)\mu_\gamma+\left(1+\sqrt{\frac{1}{f}-1}\right)\Delta\right]. \tag{34}$$

The expression in (34) is positive if either of the following two conditions holds

$$f \leq \frac{1}{2} \quad \text{or} \tag{35}$$

$$f > \frac{1}{2} \quad \text{and} \quad \Delta > \Delta_2 \tag{36}$$

where

$$\Delta_2 = \frac{1-\sqrt{\frac{1}{f}-1}}{1+\sqrt{\frac{1}{f}-1}}\mu_\gamma = \frac{\sqrt{f}-\sqrt{1-f}}{\sqrt{f}+\sqrt{1-f}}\mu_\gamma. \tag{37}$$

Appendix E: Parameter space for disease persistence. We investigated the space of parameters for which the infection persists by studying the possible parameter values for which the inequality $\mathcal{R}_0 > 1$ holds. This is equivalent to having

$$\Delta^2+(1-2f)\beta\Delta+\mu_\gamma(\beta-\mu_\gamma)>0. \tag{38}$$

It is clear that the values of f and μ_γ play a crucial role in determining the sign of the expression in the left hand side of (38). On performing some analysis, we get that the inequality (38) holds if

1. $f < \frac{1}{2}$ and
   $\mu_\gamma < \beta$ or (39)
   $\mu_\gamma > \beta \& \Delta > \tilde{\Delta}_2$ (40)
2. $f > \frac{1}{2}$ and
   $\mu_\gamma < \frac{\beta}{2}\left(\sqrt{f}+\sqrt{1-f}\right)^2 := \mu_\gamma^*$ or (41)
   $\frac{\beta}{2}\left(\sqrt{f}+\sqrt{1-f}\right)^2 < \mu_\gamma < \beta$
   $\&\quad (\Delta < \tilde{\Delta}_1 \quad \text{or} \quad \Delta > \tilde{\Delta}_2)$ or (42)
   $\mu_\gamma > \beta \quad \& \quad \Delta > \tilde{\Delta}_2$ (43)

where

$$\tilde{\Delta}_1 = \frac{1}{2}\left[(2f-1)\beta - \sqrt{(2f-1)^2\beta^2 - 4\mu_\gamma(\beta-\mu_\gamma)}\right], \tag{44}$$

$$\tilde{\Delta}_2 = \frac{1}{2}\left[(2f-1)\beta + \sqrt{(2f-1)^2\beta^2 - 4\mu_\gamma(\beta-\mu_\gamma)}\right]. \tag{45}$$

It should be noted that if $f > 1/2$ and $\frac{\beta}{2}\left(\sqrt{f}+\sqrt{1-f}\right)^2 < \mu_\gamma < \beta$, then both $\tilde{\Delta}_1$ and $\tilde{\Delta}_2$ are well defined and therefore

$$\tilde{\Delta}_1 < \Delta_2 < \tilde{\Delta}_2.$$

Combining conditions (35), (36), (39), (40), (41), (42) and (43) we get Table 1 in which the domain space of parameters (for which the infection persists) and the qualitative behavior of the basic reproduction number are described. Graph examples for the different cases are shown in Figure 5.

Appendix F: Impact of recovery rate inequalities on the prevalence of infection. This section aims to answer: What is the role of recovery rates inequality on prevalence levels? The total fraction infected at the endemic equilibrium, given by $I_T^* = I_1^* + I_2^*$, can be written in terms of μ_γ and Δ as

$$I_T^* = \frac{1}{2\beta}\{\beta - 2\mu_\gamma + \sqrt{(\beta+2\Delta)^2 - 8f\beta\Delta}\}. \tag{46}$$

To study the impact of varying Δ and μ_γ on the qualitative behavior of I_T^*, we first evaluate the limit

$$\lim_{\Delta\to 0^+} I_T^* = 1 - \frac{\mu_\gamma}{\beta} = 1 - \frac{1}{\mathcal{R}_0|_{\Delta=0}} \tag{47}$$

which is positive for $\mathcal{R}_0(\Delta=0) > 1$. Hence, there are two cases, where each one is going to be studied solely.

- Case 1: $\mu_\gamma < \beta$
  In this case, we have $I_T^*(\Delta=0) > 0$. Also, we compute the derivative

$$\frac{\partial I_T^*}{\partial \Delta} = \frac{(1-2f)\beta + 2\Delta}{\beta\sqrt{(\beta+2\Delta)^2 - 8f\beta\Delta}} \tag{48}$$

  where

$$\lim_{\Delta\to 0^+} \frac{\partial I_T^*}{\partial \Delta} = \frac{1-2f}{\beta}. \tag{49}$$

  The expression in the right hand side of (49) is positive if and only if $f < \frac{1}{2}$, while otherwise it is negative. This implies that the prevalence of infection I_T^* initially increases in Δ if $f < \frac{1}{2}$ and it reaches its maximum at $\Delta = \mu_\gamma$. However, if we assume that $f > \frac{1}{2}$, then I_T^* decreases initially in Δ. It has an absolute minimum at $\Delta = \Delta^*$, where

$$\Delta^* = \left(f - \frac{1}{2}\right)\beta \tag{50}$$

  and is given by

$$I_T^*(\Delta^*) = \frac{1}{2}(\sqrt{f}+\sqrt{1-f})^2 - \frac{\mu_\gamma}{\beta}. \tag{51}$$

This absolute minimum is feasible (in the sense that $I_T^*(\Delta^*) > 0$) if and only if

$$\mu_\gamma < \frac{\beta}{2}(\sqrt{f} + \sqrt{1-f})^2 := \mu_\gamma^*. \tag{52}$$

Hence, if (52) holds, then I_T^* decreases initially till reaching its minimum at $\Delta = \Delta^*$ and then increases to reach its maximum at $\Delta = \mu_\gamma$. However, if the inequality (52) is reversed, i.e., $\mu_\gamma^* < \mu_\gamma < \beta$, then $I_T^*(\Delta^*) < 0$ and therefore, there are two non-connected phases for the domain of definition of I_T^*, which correspond to those for which $R_0(\Delta) > 1$ and are given by $\Delta \in [0, \tilde{\Delta}_1]$ and $\Delta \in [\tilde{\Delta}_2, \mu_\gamma]$. On the first phase, I_T^* is decreases till vanishing at $\Delta = \tilde{\Delta}_1$, while on the second one I_T^* increases in till reaching its maximum at $\Delta = \tilde{\Delta}_2$.

- Case 2: $\mu_\gamma > \beta$
  In this case $I_T^*(\Delta = 0) < 0$. Thus, I_T^* is well defined only if $\Delta \in [\tilde{\Delta}_2, \mu_\gamma]$. It is easy to check that

$$\lim_{\Delta \to \tilde{\Delta}_2^+} \frac{\partial I_T^*}{\partial \Delta} = \frac{\sqrt{(\beta - 2\mu_\gamma)^2 - 4f(1-f)\beta^2}}{\beta(2\mu_\gamma - \beta)} > 0. \tag{53}$$

  This implies that I_T^* is increasing on its domain of definition.

Table 2 and figure 7 summarize the qualitative behavior in these different cases.

Appendix G: Impact of increasing ν on the qualitative behavior of $\mathcal{R}_0$. What is the effect of increasing the variance ν on $\mathcal{R}_0$? To find that out, we compute $\frac{\partial \mathcal{R}_0}{\partial \nu}$ [3]. Thus,

$$\frac{\partial \mathcal{R}_0}{\partial \nu} = \frac{\beta}{2}\sqrt{\frac{f(1-f)}{\nu}}\left(\left(\mu - \sqrt{\frac{f\nu}{1-f}}\right)^{-2} - \left(\mu + \sqrt{\frac{(1-f)\nu}{f}}\right)^{-2}\right). \tag{54}$$

Now, since

$$\sqrt{\frac{(1-f)\nu}{f}} + \sqrt{\frac{f\nu}{1-f}} > 0$$

then

$$\mu + \sqrt{\frac{(1-f)\nu}{f}} > \mu - \sqrt{\frac{f\nu}{1-f}}.$$

I.e.,

$$\left(\mu - \sqrt{\frac{f\nu}{1-f}}\right)^{-2} > \left(\mu + \sqrt{\frac{(1-f)\nu}{f}}\right)^{-2}$$

Hence, for $\nu > 0$, the expression in the right hand side of (54) is always positive. Moreover, it can be easily checked that

$$\lim_{\nu \to 0^+} \frac{\partial R_0}{\partial \nu} = \frac{\beta}{\mu^3}. \tag{55}$$

Thus,

$$\frac{\partial \mathcal{R}_0}{\partial \nu} > 0$$

[3] It is prudent to remark that the change in $\nu(\gamma_1, \gamma_2, f)$ in this partial derivative can only be due to changes in γ_1 and γ_2, not in f, given that f is held constant in the rest of the expression for $\mathcal{R}_0$.

irrespective of the value of both μ and f.

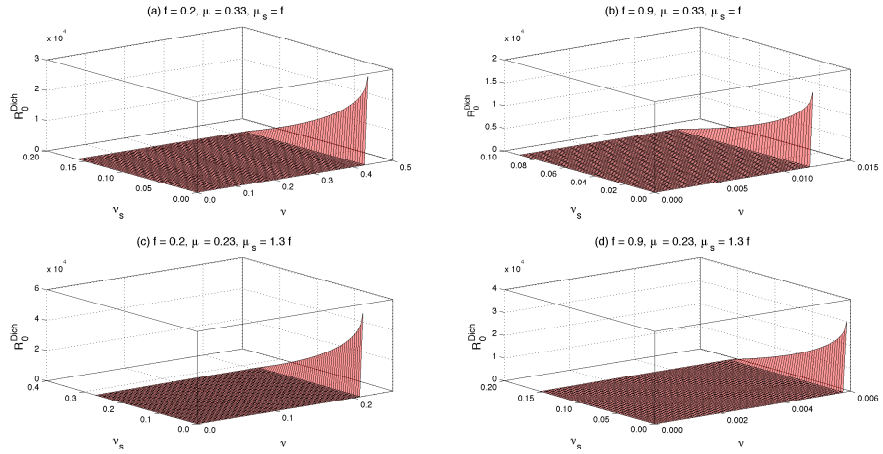

FIGURE 8. The basic reproduction number R_0^{Dich} for the dichotomous susceptible population model (56) as a function of the variance in recovery rates ν and the variance in susceptibility ν_s. Simulations have been done for $\bar{\beta} = 3$, while the value of the parameters f, μ_s and μ are as shown on the subfigures.

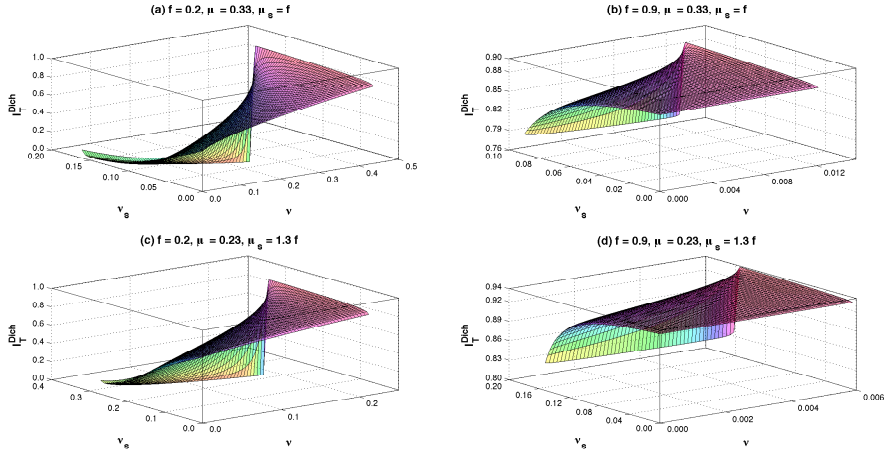

FIGURE 9. The endemic prevalence of infection I_T^{Dich} for the dichotomous susceptible population model (56) as a function of the variance in recovery rates ν and the variance in susceptibility ν_s. Simulations have been done for $\bar{\beta} = 3$, while the value of the parameters f, μ_s and μ are as shown on the subfigures.

Appendix H: Model for two dichotomous susceptible populations. Model (1) in the main manuscript could be generalised to include dichotomous susceptible

populations by assuming that the susceptibility of individuals in the group with higher healthcare facilities to be g_1 and that of the other group to be g_2, with $g_2 > g_1$. We further assume that $\bar{\beta}$ is the average number of contacts per unit time. Thus, the modified version of model (1) in the main manuscript reads

$$\begin{aligned} \frac{dI_1}{dt} &= g_1\bar{\beta}(f - I_1)(I_1 + I_2) - \gamma_1 I_1, \\ \frac{dI_2}{dt} &= g_2\bar{\beta}[(1-f) - I_2](I_1 + I_2) - \gamma_2 I_2. \end{aligned} \tag{56}$$

The connection between both models (1) in the main manuscript and (56) is that if we assume both susceptibilities to be equal (i.e., $g_1 = g_2 = g$ (say), then $g\bar{\beta} = \beta$ is the successful contact rate and, hence, we get model (1) again. Moreover, the analysis of model (56) is similar to that of (1), where the results could be obtained by replacing each β, γ_1 and γ_2 with $\bar{\beta}, \gamma_1/g_1$ and γ_2/g_2 respectively. Hence, the new basic reproduction number reads

$$\mathcal{R}_0^{Dich} = \bar{\beta}\left(\frac{g_1 f}{\gamma_1} + \frac{g_2(1-f)}{\gamma_2}\right). \tag{57}$$

On considering the weighted mean (μ_s) and variance (ν_s) in susceptibility, then we get

$$\mu_s = f g_1 + (1-f)g_2, \qquad \nu_s = f(g_1 - \mu_s)^2 + (1-f)(g_2 - \mu_s)^2$$

Solving for g_1 and g_2 from these two expressions yields:

$$g_1 = \mu_s + \sqrt{\frac{(1-f)\nu_s}{f}}, \qquad g_2 = \mu_s - \sqrt{\frac{f\nu_s}{(1-f)}}. \tag{58}$$

Since $g_2 \geq 0$, the variance must satisfy $\nu_s \leq \mu_s^2(1-f)/f := \nu_s^{max}$. Now, we use (6) and (58) in (59) to get the basic reproduction number for the dichotomous susceptible population model as

$$\mathcal{R}_0^{Dich} = \bar{\beta}\left(\frac{\mu_s\sqrt{f} + \sqrt{(1-f)\nu_s}}{\mu\sqrt{f} + \sqrt{(1-f)\nu}} f + \frac{\mu_s\sqrt{1-f} - \sqrt{f\nu_s}}{\mu\sqrt{1-f} - \sqrt{f\nu}}(1-f)\right). \tag{59}$$

Extensive simulations have been performed to study the dependence of R_0^{Dich} on the variances in recovery rates ν and in susceptibilities ν_s. Figure 8 shows that the basic reproduction number for the model with two dichotomous susceptible population increases with the increase in the recovery rates variance ν, while it decreases with the increase in the susceptibility variance ν_s. The figure is drawn for fixed value of the average contact rate $\bar{\beta}$ and different values of the means μ, μ_s and the proportion f of the population who have higher healthcare access.

The equilibrium analysis shows that endemic prevalence I_T^* for the dichotomous susceptible population model (56) reads

$$\begin{aligned} I_T^{Dich} &= \frac{1}{2\bar{\beta}}\left[\bar{\beta} - \left(\frac{\gamma_1}{g_1} + \frac{\gamma_2}{g_2}\right)\right] + \\ &\frac{1}{2\bar{\beta}}\sqrt{\left[\bar{\beta} - \left(\frac{\gamma_1}{g_1} + \frac{\gamma_2}{g_2}\right)\right]^2 + 4\bar{\beta}\left[(1-f)\frac{\gamma_1}{g_1} + f\frac{\gamma_2}{g_2}\right] - 4\frac{\gamma_1}{g_1}\frac{\gamma_2}{g_2}}. \end{aligned} \tag{60}$$

On using (6) and (58) in (60), we get

$$I_T^{Dich} = \frac{1}{2\bar{\beta}}\left[\bar{\beta} - \left(\frac{\mu\sqrt{f} + \sqrt{(1-f)\nu}}{\mu_s\sqrt{f} + \sqrt{(1-f)\nu_s}} + \frac{\mu\sqrt{1-f} - \sqrt{f\nu}}{\mu_s\sqrt{1-f} - \sqrt{f\nu_s}}\right)\right] + \frac{1}{2\bar{\beta}}\sqrt{\text{Discriminant}} \tag{61}$$

where

$$\begin{aligned}\text{Discriminant} &= \left[\bar{\beta} - \left(\frac{\mu\sqrt{f} + \sqrt{(1-f)\nu}}{\mu_s\sqrt{f} + \sqrt{(1-f)\nu_s}} + \frac{\mu\sqrt{1-f} - \sqrt{f\nu}}{\mu_s\sqrt{1-f} - \sqrt{f\nu_s}}\right)\right]^2 \\ &+ 4\bar{\beta}\left[\frac{\mu\sqrt{f} + \sqrt{(1-f)\nu}}{\mu_s\sqrt{f} + \sqrt{(1-f)\nu_s}}(1-f) + \frac{\mu\sqrt{1-f} - \sqrt{f\nu}}{\mu_s\sqrt{1-f} - \sqrt{f\nu_s}}f\right] \\ &- 4\left[\frac{\mu\sqrt{f} + \sqrt{(1-f)\nu}}{\mu_s\sqrt{f} + \sqrt{(1-f)\nu_s}}\right]\left[\frac{\mu\sqrt{1-f} - \sqrt{f\nu}}{\mu_s\sqrt{1-f} - \sqrt{f\nu_s}}\right].\end{aligned} \tag{62}$$

The impact of increasing the variance in susceptibility is investigated numerically and the simulations are shown in figure 9. It shows that the increase in the variance ν_s implies a decrease in the endemic prevalence I_T^{Dich}. In summary, the analyses of the model with the inclusion of dichotomous susceptible population reveals that the increase in the variance in susceptibility diminishes the effects of increased variance in recovery. In other words, the effects of having less-susceptible individuals counterbalances the effects of a slow recovering infected population.

Appendix I: Effects of increasing recovery rate heterogeneity via agent-based model simulations. To address the question of how increasing of recovery rate heterogeneity translates to the levels of disease prevalence in the population, in this section we take an individual-based approach, where instead of having two groups of individuals characterized by two different recovery rates, each individual is assigned a recovery rate. The recovery rates of each individual are sampled from distributions with different properties (e.g., variance), allowing us to assess how these properties affect disease outcome. More specifically, we focus on symmetric recovery rate distributions (with fixed means), and test wether larger variance (i.e., inequality) yields larger levels of disease.

In this model, a susceptible individual becomes infected at a rate proportional to the frequency of interactions with infected individuals, and the transmission rate β.

By assuming that the transition processes from one class to another is a homogeneous Poisson process, the probability a susceptible individual becomes infected between time t and $t + dt$, namely $\mathbb{P}_I(t)$ is given by

$$\mathbb{P}_I(t) = 1 - \exp(-\beta I(t)dt/N), \tag{63}$$

where the other parameters in the transition rate are $I(t)$, the number of infected at time t, and N, the size of the population.

When infected, individuals recover at different rates, moving back to the susceptible class. We model the recovery rate as a random variable (r.v.) Γ, measured in 1/days. Let Γ_M and Γ_m be the maximum and minimum recovery rates possible, respectively. Thus the interval $[\Gamma_m, \Gamma_M]$ is the support of Γ. Let also $\Delta\Gamma = \Gamma_M - \Gamma_m$. Finally, let $\Gamma = g(X) = \Delta\Gamma X + \Gamma_m$. Here X is a Beta distributed r.v. with probability density function given by $f_B(x, a, b)$ with parameters a and b. Since

the function g is monotonic, then the density function for the r.v. Γ, with random realization γ, is given by

$$f_\Gamma(\gamma) = \left| \frac{d}{d\gamma}(g^{-1}(\gamma)) \right| \cdot f_B(g^{-1}(\gamma)) = \frac{1}{\Delta\Gamma} f_B\left(\frac{\gamma - \Gamma_m}{\Delta\Gamma}, a, b \right), \tag{64}$$

where g^{-1} denotes the inverse function.

Using the Beta distribution as a kernel for the recovery rates Γ, allows for the shape of this distribution to be considered a descriptive proxy for the structure of inequalities in the population. Different inequality profiles– that is, distribution profiles– can be easily obtained by calibrating the parameters in the distribution, making this theoretical framework quite flexible to test the effects of different inequality profiles on epidemic outcomes.

In the simulations, once a recovery rate, namely γ_i, has been assigned to the ith agent, its corresponding time of infection is computed as $1/\gamma_i$, that is, the expected infectious period given that its infectious period is exponentially distributed with rate γ_i. In other words, the ith agent, once infected, spends $1/\gamma_i$ days in the infectious class. Noteworthy, the distribution of infectious periods does not necessarily share the same symmetry properties as that of the recovery rates. In fact, when the recovery rates are symmetrically distributed, the distribution of infectious periods tend to be skewed to the right.

The Beta distribution and Inequalities. Let the random variable X follow a Beta distribution, with $0 \leq X \leq 1$, and shape parameters $a > 0$ and $b > 0$. Its mean and variance are given, respectively, by

$$\mu_B = \frac{a}{a+b}, \qquad \sigma_B = \frac{ab}{(a+b)^2(a+b+1)}. \tag{65}$$

Suppose μ_B is fixed at a constant value m. Then its variance can be calibrated with only one of the parameters, say a. Deriving $b(\mu_B) = a(1-\mu_B)/\mu_B$ from the expression of the mean in (65), and substituting in the expression for the variance, we get

$$\sigma_B(a|\mu_B = m) = \frac{(m-1)m^2}{a+m} \tag{66}$$

and it can be shown that increasing the parameter a when the mean is fixed decreases the variance of the distribution. Figure 10 shows the conduciveness of this distribution for testing different inequalities scenarios, from large inequality where most individuals either recover rapidly or very slowly(top left panel), to relatively small inequality (bottom right panel).

Simulations. The simulations were set up as follows. The variance of the recovery period distribution is controlled by parameter a, which took the values 0.1,0.2,0.5,1,2,5,10,20 and 50. To explore the role of mean of the recovery rates, four combinations of maximum and minimum recovery rates were used, with the corresponding values of $\Gamma_m = \{1/60, 1/60 + 0.01, 1/60 + 0.03, 1/60 + 0.05\}$ and $\Gamma_M = \{1/5, 1/5 + 0.01, 1/5 + 0.03, 1/5 + 0.05\}$. These rendered, respectively, mean recovery rates of 0.11, 0.12, 0.14 and 0.16.

To investigate the role of pathogen transmissibility, the transmission rate β is also varied, taking up values 0.11, 0.13 and 0.15. The population size was $N = 10^5$.

For each parameter combination, 20 simulations were run for 100 days, with a time step of $dt = 0.1$ (1000 time iterations). At the beginning of each run, 5 individuals were infected. The recovery rate of each agent was assigned at the start

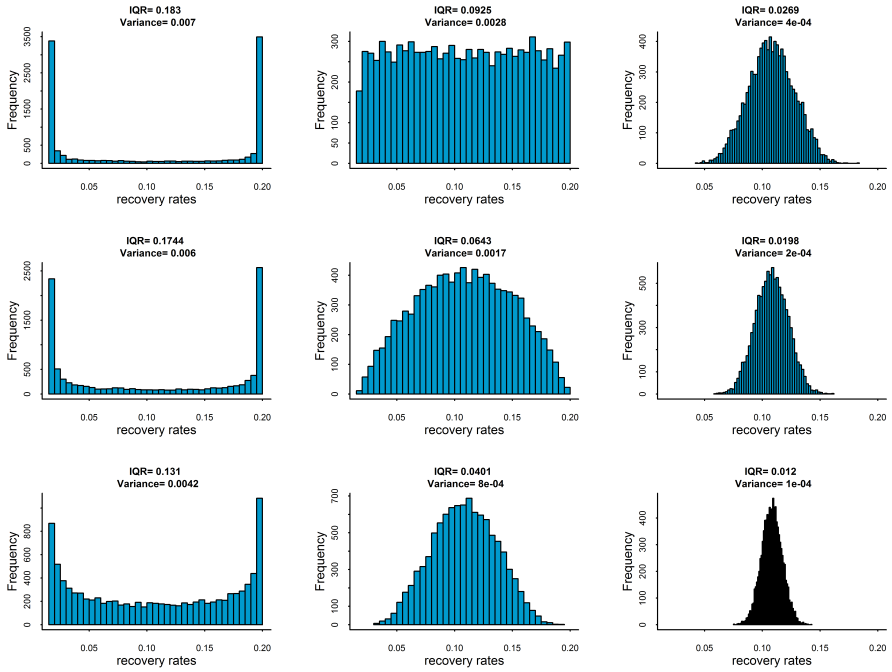

FIGURE 10. Sampling 10000 r.v. from f_Γ with maximum recovery rate of $\Gamma_M = 1/5$ and minimum of $\Gamma_m = 1/60$, and $\mu_B = 0.5$. Each panel depicts the interquantile and variance of each distribution.

of each simulation run (even for those individuals that never got infected). These rates were sampled from the corresponding distributions determined by parameters a, Γ_M, Γ_m, and $\mu_B = 0.5$ (the mean was fixed in order to yield symmetric distributions). The infectious period of each agent is given by the inverse of their respective recovery rates.

For each run (1000 iterations), the prevalence is computed as the mean of the prevalence values over the last 100 iterations conditional on non extinction. That is, we take averages over those iterations that led to endemic levels of the disease, discarding the epidemic dies-out. Since population size does not change, we report prevalence as fractions of the population infected. Finally for each parameter value, we plot the mean of prevalences over the 20 simulations, along with the standard errors, versus the variance of the corresponding recovery rates distributions. In addition, as suggested by the reviewer, we reported the results in terms of the median and the interquartile range (IQR), a nonparametric equivalent of the variance.

Results. Figures 11 and 12 show that the prevalence increases along with the variance and the IQR of the recovery rates. However, the rate of increase is different for different transmission rates and different mean recovery rates. To form an idea regarding the effect of these two quantities on the relation between variance and prevalence, for each pair of values of these two quantities, we divide the mean prevalence at the highest variance by the mean prevalence at the lowest variance. This ratio gives us an estimate of the rate at which prevalence increases with respect to the variance, that is, the partial derivative $r_\nu = \partial I(t)/\partial \nu$.

These calculations suggest that as the transmission rate increases, the estimates of r_ν decrease. Put differently, the effect of the variance of the recovery rates on the prevalence is larger for less transmissible diseases. Additionally, we find that as the mean recovery rate increases, the estimates of r_ν also increase. In other words, the effect of the variance on the prevalence is larger when individuals recover faster on average.

Noting that the reproduction number for a simple SIS model as the one studied herein is given by β/μ, with $1/\mu$ being the (mean) recovery rate, these two observations can be synthesized as: the effect of the variance of the recovery rates on disease prevalence increase as the spreading potential of the disease decreases.

Finally, we must note that one key limitation is that recovery times are exponentially distributed, an assumption that is known not to hold empirically. Moreover, this stochastic model gave us some insight into a factor contributing to the observation that larger disease prevalence follows larger variance of recovery rates. Even though the recovery rates were symmetrically distributed, the recovery times were skewed to the right, as noted before. Furthermore, as the variance of the recovery rates decreases so does the variance of the recovery times, but also the mean of the recovery times decreases, with these faster recovery times leading to lower disease prevalence. This could be partly accountable for the relation we observe between variance and prevalence. Consequently, we believe this issue should be further explored relaxing the exponentially distributed times assumption.

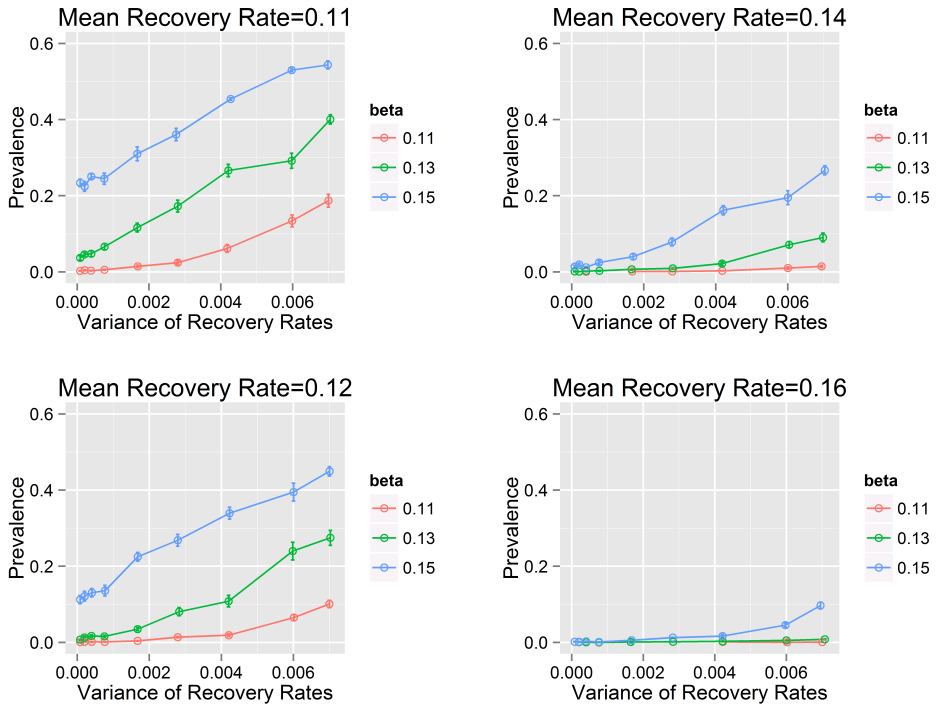

FIGURE 11. Mean and standard error (bars) infection prevalence versus Variance for different values of the mean recovery rate and the transmission rate.

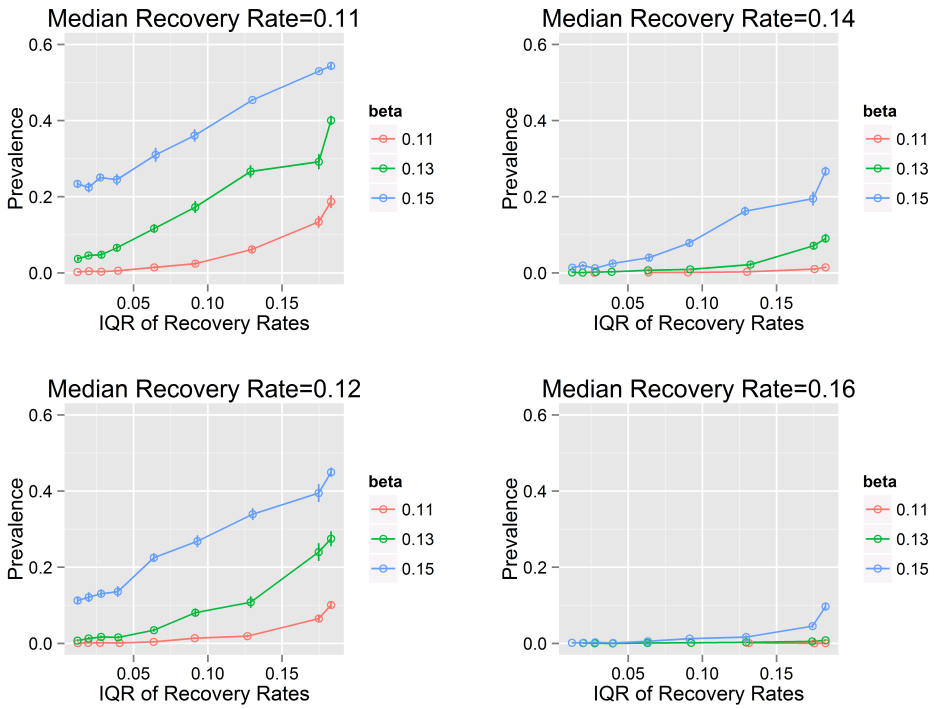

FIGURE 12. Mean and standard error (bars) of infection prevalence versus IQR for different values of the mean recovery rate and the transmission rate.

REFERENCES

[1] E. Alirol, L. Getaz, B. Stoll, F. Chappuis and L. Loutan, Urbanisation and infectious diseases in a globalised world, *The Lancet Infectious Diseases*, **11** (2011), 131–141.

[2] L. J. Allen, *An Introduction to Stochastic Processes with Applications to Biology*, 2^{nd} edition, Pearson Education, New Jersey, 2003.

[3] J. P. Aparicio, A. F. Capurro and C. Castillo-Chávez, Markers of disease evolution: The case of tuberculosis, *Journal of Theoretical Biology*, **215** (2002), 227–237.

[4] P. H. Bamaiyi, The role of demographics and human activities in the spread of diseases, *Current Trends in Technology and Sciences*, **2** (2013), 253–257.

[5] S. P. Blythe and C. Castillo-Chavez, Like-with-like preference and sexual mixing models, *Mathematical Biosciences*, **96** (1989), 221–238.

[6] F. Brauer and C. Castillo-Chavez, *Mathematical Models in Population Biology and Epidemiology*, Springer, 2012.

[7] C. Castillo-Chavez, W. Huang and J. Li, Competitive exclusion in gonorrhea models and other sexually transmitted diseases, *SIAM Journal on Applied Mathematics*, **56** (1996), 494–508.

[8] C. Castillo-Chavez, W. Huang and J. Li, The effects of females' susceptibility on the coexistence of multiple pathogen strains of sexually transmitted diseases, *Journal of Mathematical Biology*, **35** (1997), 503–522.

[9] C. Castillo-Chavez, W. Huang and J. Li, Competitive exclusion and coexistence of multiple strains in an SIS STD model, *SIAM Journal on Applied Mathematics*, **59** (1999), 1790–1811.

[10] C. Castillo-Chavez and B. Song, Dynamical models of tuberculosis and their applications, *Math. Biosci. Eng.*, **1** (2004), 361–404.

[11] A. Chen, E. Oster and H. Williams, *Why is Infant Mortality Higher in the US than in Europe?*, National Bureau of Economic Research, 2014.

[12] K. C. Chow, X. Wang and C. Castillo-Chavez, A mathematical model of nosocomial infection and antibiotic resistance: Evaluating the efficacy of antimicrobial cycling programs and patient isolation on dual resistance, Mathematical and Theoretical Biology Institute archive, 2007.

[13] C. Cohen, D. Horlacher and F. L. MacKellar, Is urbanization good for a nation's health, 2010. Available from: http://epc2010.princeton.edu/papers/100012.

[14] C. Dye, Health and urban living, *Science, American Association for the Advancement of Science*, **319** (2008), 766–769.

[15] D. N. Fisman, G. M. Leung and M. Lipsitch, Nuanced risk assessment for emerging infectious diseases, *Lancet*, **383** (2014).

[16] K. Ford and A. Norris, Sexual networks of African-American and Hispanic youth, *Sexually Transmitted Diseases*, **24** (1997), 327–333.

[17] K. Ford, W. Sohn and J. Lepkowski, American adolescents: Sexual mixing patterns, bridge partners, and concurrency, *Sexually Transmitted Diseases*, **29** (2002), 13–19.

[18] S. Galea, Urbanization, urbanicity, and health, *Journal of Urban Health*, **79** (2002), S1–S12.

[19] S. Galea, N. Freudenberg and D. Vlahov, Cities and population health, *Social Science & Medicine*, **60** (2005), 1017–1033.

[20] M. G. M. Gomes, M. Lipsitch, A. R. Wargo, G. Kurath, C. Rebelo, G. F. Medley and A. Coutinho, A missing dimension in measures of vaccination impacts, *PLoS Pathogens*, **10** (2014).

[21] T. Harpham and C. Molyneux, Urban health in developing countries: A review, *Progress in Development Studies*, **1** (2001), 113–137.

[22] H. W. Hethcote and J. A. Yorke, *Gonorrhea Transmission Dynamics and Control*, **56**, Springer, Berlin, 1984.

[23] D. R. Holtgrave and R. A. Crosby, Social capital, poverty, and income inequality as predictors of gonorrhoea, syphilis, chlamydia and AIDS case rates in the United States, *Sexually Transmitted Infections*, **79** (2003), 62–64.

[24] M. J. Keeling and P. Rohani, *Modeling Infectious Diseases in Humans and Animals*, Princeton University Press, 2008.

[25] M. J. Keeling and B. T. Grenfell, Effect of variability in infection period on the persistence and spatial spread of infectious diseases, *Mathematical Biosciences*, **147** (1998), 207–226.

[26] D. A. Leon, Cities, urbanization and health, *International Journal of Epidemiology*, **37** (2008), 4–8.

[27] J. Li, Z. Ma, S. P. Blythe and C. Castillo-Chavez, Coexistence of pathogens in sexually-transmitted disease models, *Journal of Mathematical Biology*, **47** (2003), 547–568.

[28] M. Lipsitch, T. Cohen, B. Cooper, J. M. Robins, S. Ma, L. James, G. Gopalakrishna, S. K. Chew, C. C. Tan, M. H. Samore, et al., Transmission dynamics and control of severe acute respiratory syndrome, *Science*, **300** (2003), 1966–1970.

[29] A. L. Lloyd, Realistic distributions of infectious periods in epidemic models: Changing patterns of persistence and dynamics. *Theoretical Population Biology*, **60** (2001). 59–71.

[30] A. L. Lloyd, Destabilization of epidemic models with the inclusion of realistic distributions of infectious periods, *Proceedings of the Royal Society of London. Series B: Biological Sciences*, **268** (2011), 985–993.

[31] J. O. Lloyd-Smith, S. J. Schreiber, P. E. Kopp and W. M. Getz, Superspreading and the effect of individual variation on disease emergence, *Nature*, **438** (2005), 355–359.

[32] K. Lönnroth, E. Jaramillo, B. G. Williams, C. Dye and M. Raviglione, Drivers of tuberculosis epidemics: the role of risk factors and social determinants, *Social Science & Medicine*, **68** (2009), 2240–2246.

[33] M. Marmot, Social determinants of health inequalities, *The Lancet*, **365** (2005), 1099–1104.

[34] D. M. Morens and A. S. Fauci, Emerging infectious diseases: Threats to human health and global stability, *PLoS Pathogens*, **9** (2013), e1003467.

[35] B. Morin, Variable susceptibility with an open population: A transport equation approach, preprint, arXiv:1310.1648.

[36] B. R. Morin, C. Castillo-Chavez, S.-F. Hsu Schmitz, A. Mubayi and X. Wang, Notes from the heterogeneous: **A** few observations on the implications and necessity of affinity, *Journal of Biological Dynamics*, **4** (2010), 456–477.

[37] O. Patterson-Lomba, E. Goldstein, A. Gómez-Liévano, C. Castillo-Chavez and S. Towers, Per capita incidence of sexually transmitted infections increases systematically with urban population size: A cross-sectional study, *Sexually Transmitted Infections*,**91** (2015), 610–614.

[38] K. Pickett and R. Wilkinson, *The Spirit Level: Why More Equal Societies Almost Always do Better*, London: Allen Lane, 2009.

[39] E. Saez and G. Zucman, Wealth inequality in the united states since 1913: Evidence from capitalized income tax data, *The Quarterly Journal of Economics,* **131** (2016), 519–578.

[40] C. Stephens, Healthy cities or unhealthy islands? The health and social implications of urban inequality, *Environment and Urbanization*, **8** (1996), 9–30.

[41] S. H. Strogatz, *Nonlinear Dynamics and Chaos: With Applications to Physics, Biology, Chemistry, and Engineering*, Addison-Wesley Pub., 1994.

[42] P. van den Driessche and J. Watmough, Reproduction numbers and sub-threshold endemic equilibria for compartmental models of disease transmission, *Math. Biosci.*, **180** (2002), 29–48.

[43] *United Nations, World Urbanization Prospects: The 2011 Revision*, 2012. Available from: http://www.un.org/en/development/desa/publications/world-urbanization-prospects-the-2011-revision.html.

[44] J. Wallinga and M. Lipsitch, How generation intervals shape the relationship between growth rates and reproductive numbers, *Proceedings of the Royal Society B: Biological Sciences*, **274** (2007), 599–604.

[45] R. G. Wilkinson, Socioeconomic determinants of health. Health inequalities: Relative or absolute material standards?, *BMJ: British Medical Journal*, **314** (1997), 591–595.

[46] R. G. Wilkinson and K. E. Pickett, Income inequality and population health: A review and explanation of the evidence, *Social Science & Medicine*, **62** (2006), 1768–1784.

[47] P. Zhang and P. M. Atkinson, Modelling the effect of urbanization on the transmission of an infectious disease, *Mathematical Biosciences*, **211** (2008), 166–185.

Received August 06, 2015; Accepted April 08, 2016.

E-mail address: oskkypatterson@yahoo.es
E-mail address: muntaser_safan@yahoo.com
E-mail address: smtowers@asu.edu
E-mail address: jetaylo6@asu.edu